Organization of Inorganic Nanoparticles Using Biotin−Streptavidin Connectors

Mei Li, Kim K. W. Wong, and Stephen Mann*

Department of Chemistry, University of Bath, Bath BA2 7AY, UK

Received September 2, 1998
Revised Manuscript Received November 16, 1998

The synthesis and assembly of new forms of inorganic matter organized at the nanometer and mesoscopic length scales is currently receiving much attention. Such materials are not only of intrinsic interest but might be useful in devices that exploit size- and pattern-dependent properties such as Coulomb charging in nanoelectronic digital circuits. Recent work has indicated that inorganic nanoparticles can be used as constructional units for superlattice arrays formed for example by solvent evaporation of hydrophobic inorganic colloids.[1−3] In general, colloidal crystallization results in hexagonally close-packed arrays, although alternate geometries have been achieved by using elliptically shaped particles[4] or by direct synthesis in the presence of porous bacterial membranes with oblique or square lattice symmetry.[5] Another approach has focused on the use of molecular cross-linking of self-assembled monolayers[6,7] to generate periodic and non-periodic networks of covalently linked metal nanoparticles. One potential strategy which offers much scope involves the construction of organized systems by biomolecular recognition of complementary connecting units preattached to the surfaces of inorganic nanoparticles. For example, initial studies have shown that complementary strands of DNA molecules can be used to self-assemble inorganic nanoparticles.[8−10] In this paper, we describe an alternative approach in which we use the high-affinity binding of streptavidin to biotinylated amino acid residues on the surface of a protein, ferritin, to reversibly generate networks of superparamagnetic iron oxide nanoparticles.

The iron storage protein ferritin consists of a hollow polypeptide shell, 8 and 12 nm in internal and external diameter, respectively, which is constructed from 24 symmetry-related subunits.[11] The central cavity usually contains a 5 nm diameter ferric oxide core of structure similar to that of the mineral ferrihydrite ($5Fe_2O_3 \cdot 9H_2O$). Hydrophilic and hydrophobic channels penetrate the shell, and as a result, iron atoms can be removed from the cage by reductive dissolution. Moreover, the empty cage of apoferritin can be remineralized in vitro with a range of inorganic oxides and sulfides that have controlled particle sizes.[12−15] In this work we chemically prime the surface of ferritin for controlled cross-linking with an auxiliary protein (streptavidin) by nucleophilic coupling of a succinimidyl derivative of biotin to the 60−70 exposed lysine residues (Scheme 1). A flexible hexanoate spacer is incorporated into the covalent linkage because the four high-affinity biotin binding sites ($K_d = 10^{-15}$ M)[16] are partially buried in the streptavidin molecule. Reversible cross-linking is achieved because the tetrameric structure of streptavidin provides a connecting unit for three-dimensional aggregation of the ferritin nanoparticles (Scheme 2). A similar strategy has been recently exploited in the controlled aggregation of multilamellar liposomes formed from biotinylated phospholipids[17] and patterning of metallic nanoparticles on a DNA-based template.[10]

Biotinylated derivatives of horse spleen ferritin were synthesized according to standard procedures.[18] The average number of biotinylated groups was determined as 72 per protein molecule.[19] Additions of streptavidin to give biotinylated ferritin:streptavidin mole ratios of either 1:6 or 1:8 produced turbid suspensions and yellow-brown macroscopic precipitates with clear supernatants within a few hours.[20] A transparent yellow supernatant, along with only a small amount of bulk precipitate, was observed at a stoichiometry of 1:4, suggesting that the extent of conjugation under these conditions was limited to the colloidal size range. A

* Current address of corresponding author: School of Chemistry, University of Bristol, Bristol BS8 1TS, UK.

(1) Murray, C. B.; Kagan, C. R.; Bawendi, M. G. *Science* **1995**, *270*, 1335.
(2) Vossmeyer T.; et al. *Science* **1995,** *267*, 1476.
(3) Petit, C.; Taleb, A.; Pileni, M.-P. *Adv. Mater.* **1998**, *10*, 259.
(4) Korgel, B. A.; Fitzmaurice, D. *Adv. Mater.* **1998**, *10*, 661.
(5) Shenton, W. Pum, D.; Sleytr, U. B.; Mann, S. *Nature* **1997**, *389*, 585.
(6) Brust, M.; Bethall, D.; Schiffrin, D. J.; Kiely, C. J. *Adv. Mater*, **1995**, *7*, 795.
(7) Andres, R. P.; Bielefeld, J. D.; Henderson, J. I.; Janes, D. B.; Kolagunta, V. R.; Kubiak, C. P.; Mahoney, W. J.; Osifchin, R. G. *Science*, **1996**, *273*, 1690.
(8) Alivisatos, A. P.; Johnsson, K. P.; Peng, X.; Wilson, T. E.; Loweth, C. J.; Bruchez, M. P.; Schultz, P. G. *Nature* **1996**, *382*, 609.
(9) Mirkin, C. A.; Letsinger, R. L.; Mucic, R. C.; Storhoff, J. J. *Nature* **1996**, *382*, 607.
(10) Niemeyer C. M.; Burger, W.; Peplies, J. *Angew. Chem., Int. Ed. Engl.* **1998**, *37*, 2265−2268.
(11) Harrison, P. M.; Arosio, P. *Biochim. Biophys. Acta*, **1996**, *1275*, 161.
(12) Meldrum, F. C.; Heywood, B. R.; Mann, S. *Science* **1992**, *257*, 522.
(13) Douglas, T.; Dickson, D. P. E.; Betteridge, S.; Charnock, J.; Garner, C. D.; Mann, S. *Science* **1995**, *269*, 54.
(14) Meldrum, F. C.; Douglas, T.; Levi, S.; Arosio, P.; Mann, S. *J. Inorg. Biochem.* **1995**, *8*, 59.
(15) Wong, K. K. W.; Mann, S. *Adv. Mater.* **1996**, *8*, 928.
(16) Weber, P. C.; Ohlendorf, D. H.; Wendoloski, J. J.; Salemme, F. R. *Science* **1989**, *243*, 85.
(17) Chiruvolu, S.; Walker, S.; Israelachvili, J.; Schmitt, F.-J.; Leckband, D.; Zasadzinski, J. A. *Science* **1994**, *264*, 1753.
(18) In a typical reaction, 40 μL of aqueous sodium sulfosuccinimidyl-6-biotinamidohexanoate (44.9 mM, 25 mg/mL, $C_{20}H_{29}N_4NaO_9S_2$, $M_r = 556.57$, Vector Laboratories) was added at room temperature to 5 mL of a horse spleen ferritin solution {4 μM, 2 mg/mL, $M_r = 500$ kDa (Calbiochem) buffered at pH 8.5 (100 mM HEPES [*N*-(2-hydroxyethyl)piperazine-*N*′-(2-ethanesulfonic acid)]}. The reaction solution was occasionally stirred over a period of 4 h and then dialyzed against buffer (HEPES, 2 L, 4 °C, 24 h) to remove the unreacted reagent and small molecule reaction products. The concentration of clear yellow biotinylated ferritin solutions was determined by use of a Bicinchonini Acid Protein Assay Kit (SIGMA procedure No. TPRO-562).

(19) The reaction solution containing known concentrations of biotinylated-ferritin was centrifuged (Centricon-50, MILLIPORE) and the supernatant analysed for unreacted biotin by visible spectroscopy using the dye 4-hydroxyazobenzene-2-carboxylic acid (HABA) (Green, N. M. *Methods Enzymol.* **1970**, *18A*, 418).
(20) Molecular cross-linking of the biotinylated ferritin was carried out at room temperature by addition of streptavidin [167 μM, 1.0 mg in 0.1 mL 10 mM phosphate/0.15 M NaCl buffer, pH 7.5, $M_r = 60$ kDa (Vector Laboratories)] to solutions of biotinylated ferritin. The mole ratio of biotinylated ferritin:streptavidin was varied between values of 1:2 to 1:12. Samples were left unstirred at room temperature for up to several days.

10.1021/cm980610m CCC: $18.00
Published on Web 12/19/1998

Scheme 1. Reaction Scheme for Biotinylated Ferritin [a, native horse spleen ferritin; b, sulfosuccinimidyl-6-(biotinamido)hexanoate; c, biotinylation of surface lysine residues]

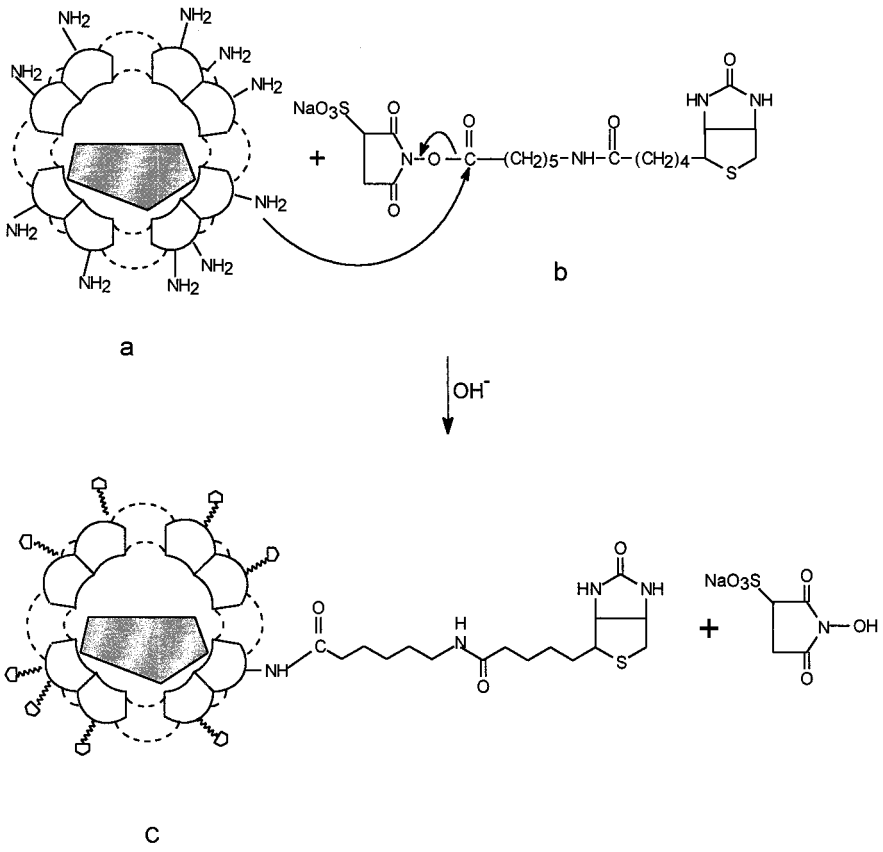

biotin-free control reaction, in which native ferritin was mixed with streptavidin in a mole ratio of 1:6, remained clear and gave no bulk precipitate. TEM images of the control sample (native ferritin + streptavidin) were similar to those recorded for native ferritin or biotinylated ferritin solutions prepared with the same protein concentration. The micrographs showed discrete electron dense iron oxide cores with occasional small aggregates due to the air-drying procedure (Figure 1a). In contrast, the streptavidin−biotinylated ferritin conjugates were extensively aggregated across the TEM grid (Figure 1b). The supramolecular aggregates were highly disordered and superlattice arrays with periodic order were not observed. Negative staining of the extended structures showed that the constituent iron oxide cores were surrounded by an intact polypeptide shell (data not shown), implying that the nanoparticle networks originate from specific intermolecular interactions between streptavidin and the surface biotinylated ligands of the modified shell of ferritin.

The strength and specificity of these interactions were confirmed by SDS−PAGE.[21] Whereas a mixture of streptavidin and native ferritin showed well-separated discrete bands, consistent with a noninteracting system, the precipitated biotinylated ferritin/streptavidin material showed no bands for the constituent proteins (Figure 2). Instead, a broad band was present in the stacking gel at the top of the lane, which corresponded to a conjugated material with significantly increased molecular weight. Although the intermolecular cross-linking was sufficiently strong to withstand disaggregation under the relatively harsh conditions used for SDS−PAGE, the thermodynamic nature of the biotin−streptavidin linkage could be used to regulate the extent of the aggregation process. For example, the reversibility of the aggregation process was demonstrated by adding a 20-fold excess (with respect to strepavidin) of free biotin to the turbid suspensions of the conjugated materials. The solutions turned clear yellow immediately, and no suspension or precipitate was observed after several days. TEM images showed that protein-encapsulated iron oxide nanoparticles were dispersed back to their original nonassociated state.

Whereas the control experiments showed no changes in turbidity over periods of several days (Figure 3a,b), turbidity curves for 1:6 mixtures of the biotinylated ferritin and streptavidin clearly indicated the formation of supramolecular aggregates and extended structures.[22] In general, the curves were characterized by an increase in turbidity to a threshold value within the first 10−15 min after mixing, followed by a discontinuous decrease due to macroscopic precipitation over periods of several hours. The first stage in this process represents the

(21) Sodium dodecyl sulfate−polyacrylamide gel electrophoresis (SDS−PAGE) was undertaken on ferritin solutions containing 0.125 M Tris buffer (pH 6.8), 4% SDS, 20% glycerol, 10% 2-mercaptoethanol, and 0.0004% bromophenol blue. The samples were loaded onto a 3% stacking gel [3% acrylamide, 0.125 M Tris pH 6.8, 0.1% TEMED (N,N,N′,N′-tetramethylethylenediamine), 0.05% ammonium persulfate] with a 7.5% separating gel (7.5% acrylamide/bisacrylamide, 0.375 M Tris pH 8.8, 0.1% SDS, 0.1% TEMED, 0.05% ammonium persulfate) and run at 120 V for 4 h with conventional cathode to anode polarity. The gel was stained with Coomassie Brilliant Blue R250 (0.25% in water/methanol/glacial acetic acid = 5:5:1 v/v) for 30 min and then destained with a water/methanol/glacial acetic acid mixure (6.5: 2.5: 1 v/v).

Scheme 2. Controlled Aggregation of Iron Oxide Nanoparticles in Biotinylated Ferritin by Streptavidin Connectors (a, biotinylated ferritin; b, streptavidin; c, organized product)

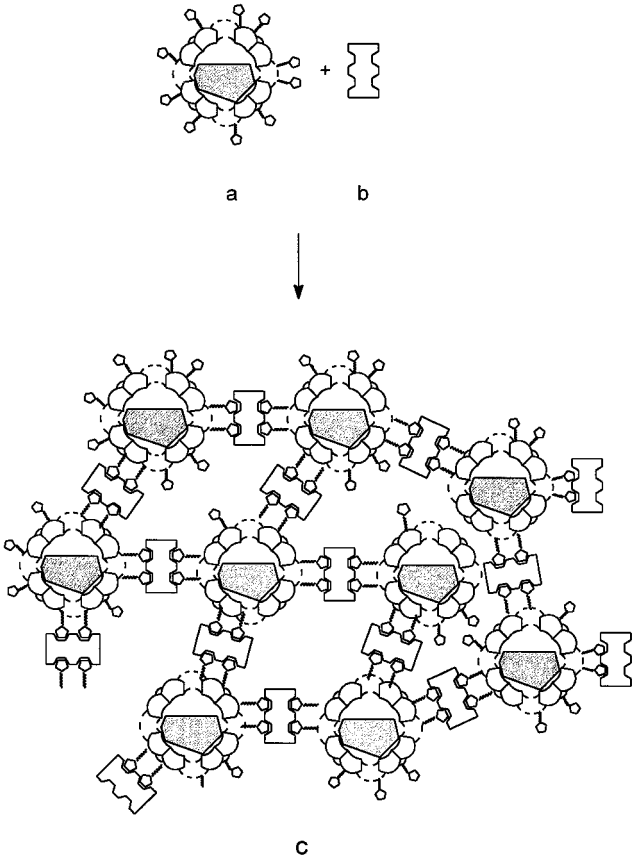

formation of supramolecular aggregates of colloidal dimensions, whereas the second stage is associated with larger extended structures that sediment under gravity. Measurements for a series of samples at a constant mole ratio of 1:6 showed that the rate of formation of the colloidal aggregates increased with the higher concentrations of biotinylated ferritin and streptavidin present in the solutions (Figure 3c−e). Similar increases in the rates of formation of ligand-induced cross-linking and associated aggregation were determined for samples in which the biotinylated ferritin to streptavidin mole ratio was increased from 1:2 up to 1:6 at a constant ferritin concentration of 0.8 μM (Figure 4a,c,e). The rate of aggregation was particularly enhanced for a 6-fold molar excess of streptavidin. Under these conditions, colloidal aggregates were rapidly formed within 10 min. Interestingly, further increases in the streptavidin concentration resulted in progressive decreases in conjugation (Figure 4d,b). Thus, although the degree of bulk precipitation observed after several hours for mixtures with a mole ratio of 1:8 was similar to that at a ratio 1:6, the rate of aggregation within the first 30 min was significantly reduced at the higher ratio. Increasing the biotinylated ferritin to streptavidin mole ratio to 1:12 gave changes in turbidity that were less pronounced than those recorded for samples prepared with the much lower ratio of 1:4.

These results indicate that the rates of formation of biotin-induced streptavidin cross-linking of ferritin molecules were dependent on the concentrations and stoichiometry of the components of the conjugated system. At ferritin to streptavidin mole ratios less than 1:4, there is insufficient streptavidin in the system to induce

(22) The change in turbidity (τ) of solutions containing various mole ratios of biotinylated ferritin and streptavidin was determined by monitoring the optical transmission ($T = I/I_o$) at 600 nm with time, using a Perkin-Elmer Lambda II UV−vis spectrometer equipped with Perkin-Elmer UV Winlab (Version 1.1) computer software. The turbidity was calculated from $\tau = -\ln(T)/l$, where l, the cell length, was equal to 1.0 cm.

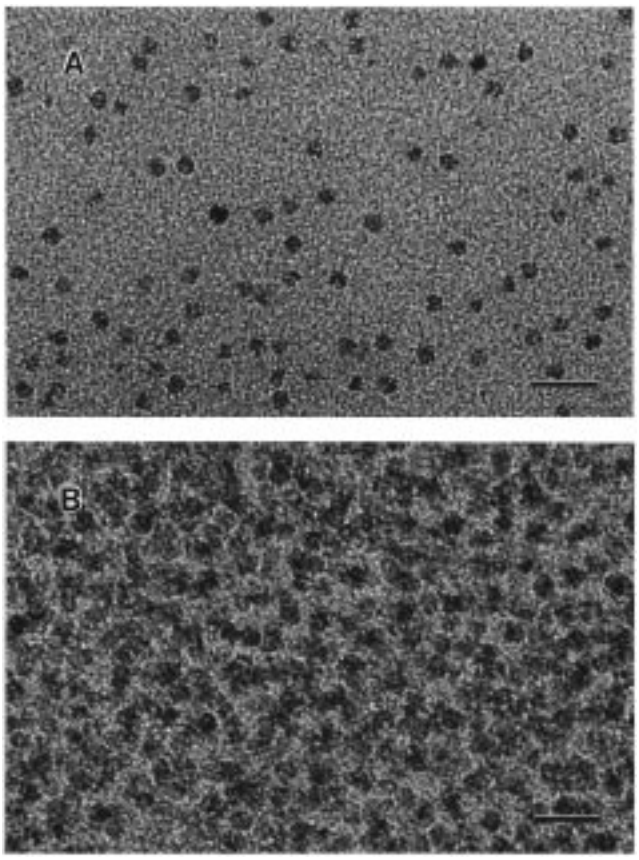

Figure 1. TEM micrographs. (a) Control experiment (addition of streptavidin to native ferritin) showing discrete electron dense iron oxide cores of nonaggregated protein molecules. (b) Aggregated network of nanoparticles formed by addition of streptavidin to biotinylated ferritin. Biotinylated ferritin: streptavidin mole ratio = 1:6 in both cases. Scale bars = 20 nm.

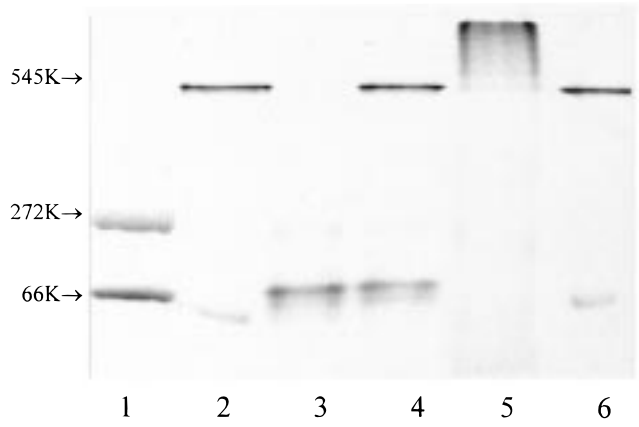

Figure 2. Coomassie Blue stained SDS−PAGE profiles: (1) protein markers, (2) native ferritin, (3) streptavidin, (4) control (native ferritin + streptavidin), (5) biotinylated ferritin + streptavidin (1:6), (6) biotinylated ferritin.

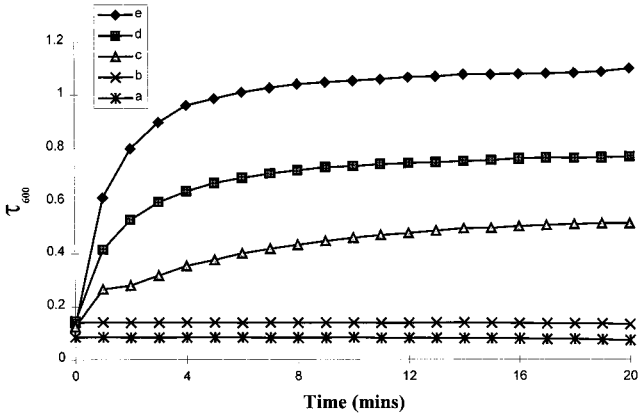

Figure 3. Initial change in turbidity at 600 nm (τ_{600}) with time after addition of streptavidin (SA) to biotinylated ferritin (BFn; ca. 72 biotin ligands per molecule) at a constant mole ratio of 6:1, respectively: (a) control, 4.8 μM SA + 0.8 μM native ferritin; (b) control, 0.8 μM BFn; (c) 2.4 μM SA + 0.4 μM BFn; (d) 3.6 μM SA + 0.6 μM BFn; and (e) 4.8 μM SA + 0.8 μM BFn.

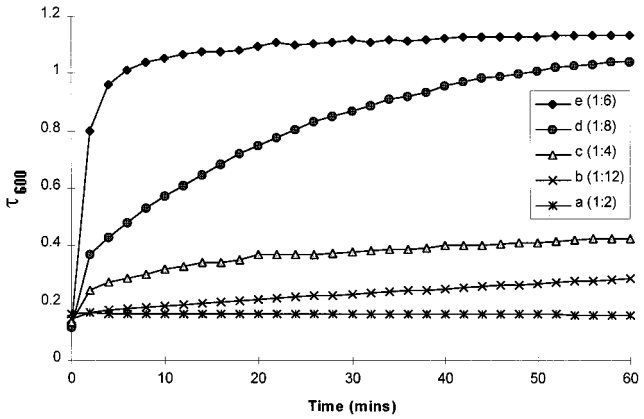

Figure 4. Change in turbidity at 600 nm (τ_{600}) with time after the addition of different amounts of streptavidin (SA) to 0.8 μM solutions of biotinylated ferritin (BFn; ca. 72 biotin ligands per molecule) to give ferritin to streptavidin mole ratios of (a) 1:2, (b) 1:12, (c) 1:4 (d) 1:8, and (e) 1:6.

the formation of extended networks of the protein-encapsulated inorganic nanoparticles. In general, the propagation of such arrays will depend not only on the concentration of streptavidin but also on the distribution and number of both free and streptavidin-bound biotinylated ligands on the surface of individual ferritin molecules in solution. As the number of biotinylated groups (72 per ferritin molecule) was significantly larger than the number of added streptavidin molecules, an excess of unbound ligands was always present in the experiments studied. However, relatively large amounts of surface-bound streptavidin could sterically block the remaining (uncoupled) ligands from participating in bridging interactions with other streptavidin−ferritin complexes. This appears to be the case at a mole ratio of 1:12, where streptavidin-coated ferritin molecules remain dispersed in solution. Moreover, the results suggest that there is an optimum stoichiometry (1:6) at which the biotinylated ferritin molecules bind sufficient numbers of streptavidin molecules without seriously compromising the cross-linking interactions. This must represent a balance between primary and secondary coupling of the biotinylated moieties to the binding sites of streptavidin and streptavidin−ferritin complexes, respectively. Apparently, these interactions become cooperative rather then competitive when approximately 10% (6/72 × 100) of the surface biotin groups are involved in primary coupling (assuming one biotinylated ligand binds to each streptavidin molecule). Whether this ratio is structurally determined, for example, by the high (cubic) symmetry of the ferritin 24-mer, which geometrically distributes the binding sites, or arises from the minimization of steric and electrostatic forces between streptavidin molecules attached to the ferritin surface is not currently known.

To conclude, we have shown that the well-known specific binding of streptavidin to biotin can be exploited in the reversible assembly of networks of protein-encapsulated inorganic nanoparticles. Ferritin is an attractive candidate for this approach because the polypeptide shell can be readily derivatized with approximately 70 biotinylated ligands that are available to interact with streptavidin to form a network of intermolecular cross-links. One potential disadvantage is that the strength and speed of the biotin−streptavidin coupling mitigates against the formation of ordered inorganic superlattices, although the use of excess amounts of nonligated biotin or soluble auxiliary molecules that competitively bind but not cross-link might counteract this. As the 8 nm internal cavity of apoferritin can be reconstituted with a variety of non-native inorganic cores, such as magnetite,[12] iron sulfide,[13] manganese oxides,[14] and cadmium sulfide,[15] it should be possible to generate nanoparticle networks consisting of other inorganic components with controllable size and composition by ligand-induced cross-linking. Moreover, because encapsulation of the inorganic phase within the protein cage restricts the length scale of particle−particle interactions and prevents direct physical contact, particle fusion, and growth within the organized phase, ferritin-based arrays could have important applications in magnetic storage and nanoelectronic devices.

CM980610M